Research Article

For reprint orders, please contact: reprints@futuremedicine.com

Nanomedicine

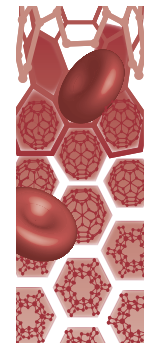

Surviving nebulization-induced stress: dexamethasone in pH-sensitive archaeosomes

Aim: To increase the subcellular delivery of dexamethasone phosphate (DP) and stability to nebulization stress, pH-sensitive nanoliposomes (LpH) exhibiting archaeolipids, acting as ligands for scavenger receptors (pH-sensitive archaeosomes [ApH]), were prepared. **Materials & methods:** The anti-inflammatory effect of 0.18 mg DP/mg total lipid, 100–150 nm DP-containing ApH (dioleylphosphatidylethanolamine: *Halorubrum tebenquichense* total polar archaeolipids:cholesteryl hemisuccinate 4.2:2.8:3 w:w) was tested on different cell lines. Size and HPTS retention of ApH and conventional LpH (dioleylphosphatidylethanolamine:cholesteryl hemisuccinate 7:3 w:w) before and after nebulization were determined. **Results & conclusion:** DP-ApH suppressed IL-6 and TNF-α on phagocytic cells. Nebulized after 6-month storage, LpH increased size and completely lost its HPTS while ApH3 conserved size and polydispersity, fully retaining its original HPTS content.

First draft submitted: 15 April 2016; Accepted for publication: 23 June 2016; Published online: 28 July 2016

Keywords: lung • macrophages targeting • nebulization • subcellular delivery

Maria Julia Altube[1], Solange Mailen Selzer[1], Marcelo Alexandre de Farias[2], Rodrigo Villares Portugal[2], Maria Jose Morilla[1] & Eder Lilia Romero*[,1]

[1]Nanomedicine Research Program, Departamento de Ciencia y Tecnología, Universidad Nacional de Quilmes. Roque Saenz Peña 352, Bernal B1876BXD, Argentina

[2]Brazilian Nanotechnology National Laboratory, CNPEM, Caixa Postal 6192, CEP 13.083–970, Campinas, São Paulo, Brazil

*Author for correspondence:
Tel.: +54 114 365 7100
Fax: +54 114 365 7132
elromero@unq.edu.ar

The inhalatory route gives the most direct access to the gas exchange surface of the lungs. This route is used for systemic drug delivery, where the drugs enter the blood by crossing the thin interface of the alveolar epithelial-vascular endothelia, or for site-specific drug delivery, to the alveoli in the lower airways.

The inhaled corticosteroids (ICs) in combination with broncodilators (selective β agonists engineered for a prolonged activity) are the first-line therapy in all patients with persistent asthma [1]. ICs are also employed to avoid the exacerbations of severe chronic obstructive pulmonary disease [2,3]. The IC are highly potent (measured as receptor affinity) hydrophobic drugs compared with dexamethasone [4]. IC at low doses have less chances of entering the blood, resulting safer and with less systemic side effects than systemic corticosteroids [5]. The systemic absorption of IC is minimized because of their low oral bioavailability and low absorption of the dose deposited in the lower airways. The IC have to exhibit also high pulmonary bioavailability, and a long pulmonary retention time. Because of these reasons, the effect exerted by an IC depends on its chemistry and its efficacy is influenced by its deposition in the airways, a fact governed by the type of delivery device [1].

Despite the meaningful advantages associated with the advent of IC, the inhaled therapies may evolve toward more refined products. The inhaled particulate carriers, for instance, are proposed to maximize the residence time in the lungs and protect the chemical structure of drugs [6]. The performance of a large variety of inhaled nanoparticulate carriers has been preclinically tested for lung delivery of corticosteroids, antitumorals and antibiotics [7]. Because of the volume of know-how gained in the last 20 years on robust manufacturing processes and the availability of high-quality excipients, now the lipid

Future Medicine part of fsg

vesicles (liposomes and nanoliposomes) are developed with acceptable chemical and physical stabilities to support meaningful pharmaceutical shelf lives [8]. This is why, despite the universe of nanoparticles in preclinical studies, liposomes and the related structures are micro/nanocarriers, mostly accepted by the pharmaceutical industry [9]. Most of the liposomes in pharmaceutical use are intended for parenteral route of administration [10,11]. Today, there are no inhaled nanoliposomes available in the market, but two inhaled liposomal formulations for amikacin (Arikayce®) and ciprofloxacin (Pulmaquin) are in late-stage clinical trials [12–15].

Pulmonary delivery poses a challenge due to the anatomic complexity of the human respiratory system. In the same way as IC, the performance of inhaled liposomes depends on the inhaler device. The most established inhalation devices for delivery of liposomes are nebulizers, since they are suited best to transport large amounts of aqueous solutions to the lungs [14].

These inhaled carriers for site-specific drug delivery may yet evolve toward more sophisticated nanoparticles displaying new functionalities, compatible with their industrial manufacture. It would be desirable, for instance, to count on carriers enabling the drugs to be delivered to a specific subcellular site (tertiary targeting) [15]. Once endocytosed, classical nanocarriers remain trapped within endo/phagocytic vesicles of growing acidity, where end up is destroyed. Because of that, unless the site of drug action is in the endolysosomes, escaping the endocytic machinery is required for drugs to target cytoplasmic or nuclear sites. That is the case of corticosteroids having cytoplasmic receptors.

In this work, we hypothesize that the performance of nebulizable corticosteroids could be improved if specifically designed carriers, such as pH-sensitive nanoliposomes (LpH), are employed.

Different types of LpH can be prepared from specific combinations of lipids or lipids and pH-sensitive polymers [16,17]. A classical composition is dioleylphosphatidylethanolamine (DOPE):cholesteryl hemisuccinate (CHEMS) (7:3 w:w). DOPE is an inverted cone-shaped lipid that forms inverted micellar phase. CHEMS consists of succinic acid esterified to the β-hydroxyl group of cholesterol, which results in the ability of CHEMS to adopt a lamellar organization upon hydration in neutral or alkaline aqueous media. By combining negatively charged CHEMS with positively charged DOPE in neutral media, a bilayer is stabilized by electrostatic interaction. When the negative charge of CHEMS is neutralized in acid media, the electrostatic association with DOPE decays. As a result, DOPE returns to its original fusogenic hexagonal Phase II. Once endocytosed, DOPE:CHEMS LpH experience a phase transition from lamellar to hexagonal Phase II triggered by the acidity of the endo/phagocytic pathway. The hexagonal Phase II fuses with the endo–lysosomal bilayers ending up with the release of carried drug to the cytoplasm.

A great deal of preclinical data have been gathered on inhaled (mostly nebulized) non-pH-sensitive liposomes [14] and on intravenous LpH [17]. Nonetheless, there is no data about nebulized LpH.

Having said that, we will finally refer to the archaeosomes (ARC). The ARC are lipid vesicles made of total polar archaeolipids (TPA) extracted from hyperhalophilic Archaebacteria *Halorubrum tebenquichense*. The archaeolipids composing the ARC are *sn*1,2 glycerol ether having fully saturated polyisoprenoid chains that make the archaeolipids resistant to lipolytic enzymes, hydrolytic or oxidative attacks [18]. ARC display typical features that distinguish them from classical liposomes prepared with phospholipids extracted from Eukaria and Bacteria domains organism. Different from liposomes, besides of a higher chemical stability the ARC poses a higher stability against detergents and physical stress (heat, lyophilization) [caimi at, parra f, de farias ma *et al.* ready to use ultradeformable nanovesicles as adjuvant for topical vaccination. *coll. surf. b.* (2016); submitted manuscript]. Previous studies have shown that ARC and related structures are more extensively captured by macrophages than conventional liposomes [19]. The inclusion of archaeolipids to an LpH may result in nanoliposomes exhibiting new pharmacodynamic properties. Ordinarily, to access the cytoplasmic receptor the corticosteroids have to diffuse across the cell membrane. Endocytosed within properly engineered carriers, the corticosteroids would enter the cytoplasm even in the absence of a huge concentration gradient. The endocytic machinery thus may account for therapeutic subcellular concentrations of corticosteroids given at low doses (Supplementary Figure 1). The presence of TPA may also increase the mechanical stability of the bilayer during nebulization, which is responsible for the loss of the liposomal drug. In this work, we describe the design and test the performance of mixed nanoliposomes DOPE:TPA:CHEMS for nebulization of the model corticosteroid dexamethasone phosphate (DP) to alveolar macrophages and alveolar epithelial cells involved in asthma inflammation [20]. DP was used instead of classical IC, because the hydrophobic drugs partitioned in the bilayer of an LpH are not efficiently released in response to the acidity [21].

Materials & methods

Materials

Soybean phosphatidylcholine (purity >90%) was a gift from Lipoid (Ludwigshafen, Germany).

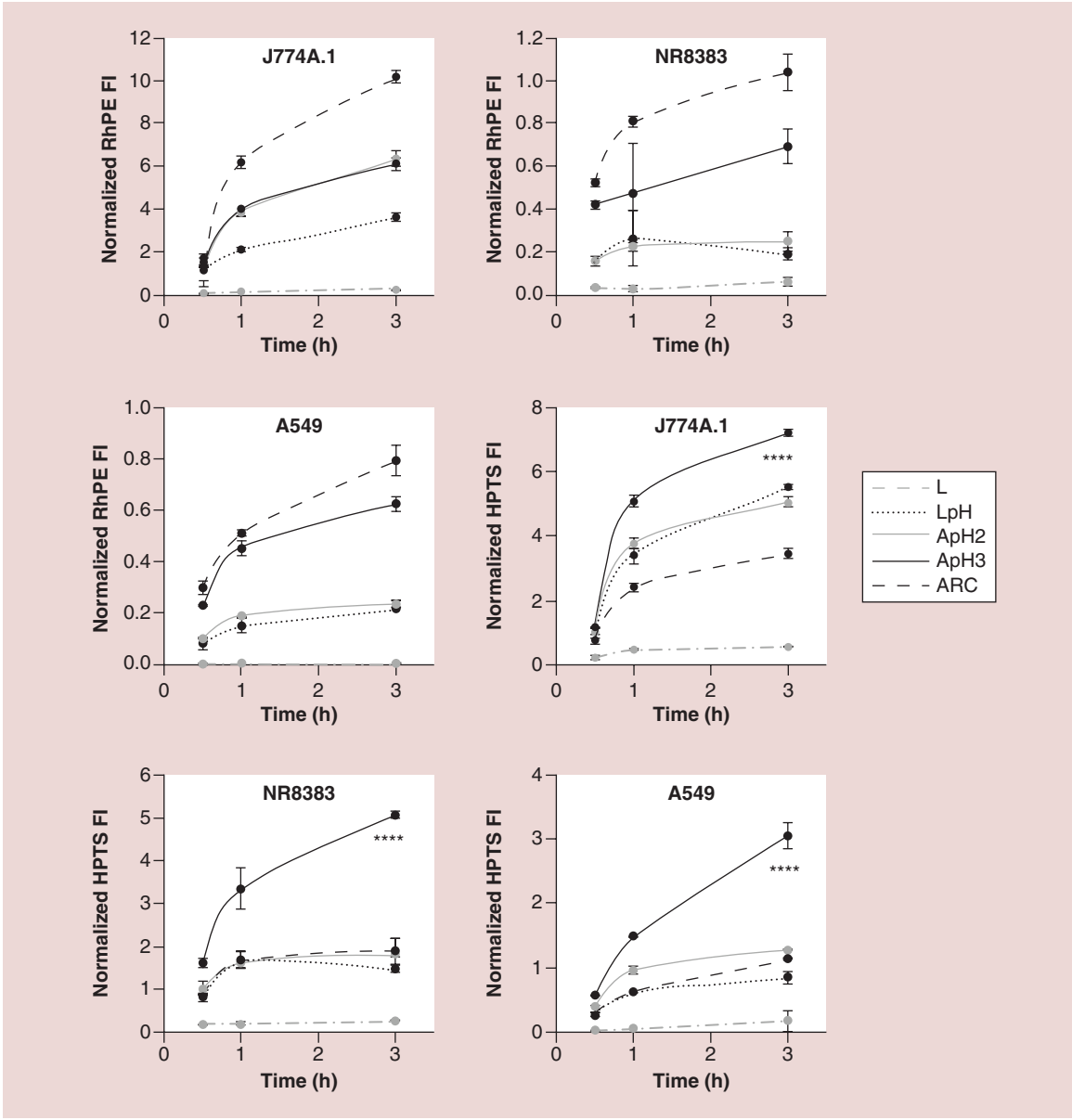

Figure 1. *In vitro* cellular uptake and subcellular pH sensitivity. Normalized RhPE and HPTS FI) of J447A.1, NR8383 and A549 cells after 0.5, 1 and 3 h of incubation with double-labeled RhPE and HPTS-DPX nanoliposomes. Values are expressed as mean ± SD (n = 3 batches).
DPX: P-xylene-bis-pyridinium bromide; FI: Fluorescence intensity; HPTS: 8-hydroxypyrene-1,3,6-trisulfonic acid trisodium salt; RhPE: rhodamine B 1,2-dihexadecanoyl-sn-glycero-3-phosphoethanolamine triethylammonium salt; SD: Standard deviation.

1,2-Hydrogenated-L-α-phosphatidylcholine (HSPC) was from Northern Lipids, Inc., Vancouver, Canada; dioleoyl-sn-glycero-3-phosphoethanolamine (DOPE) was from Avanti Polar Lipids (AL, USA); Lissamine™ rhodamine B 1,2-dihexadecanoyl-sn-glycero-3-phosphoethanolamine triethylammonium salt (RhPE) was purchased from Thermo Fisher Scientific (MA, USA); p-xylene-bis-pyridinium bromide (DPX) was from Invitrogen (OR, USA); and 5-(and-6)-chloromethyl-2′,7′-dichlorodihydrofluorescein diacetate, acetylester (carboxy-H2DCFDA), was from Molecular Probes (OR, USA). L-α-phosphatidyl-l-serine (PS), polyinosinic acid (5′) potassium (poly-I), polycytidylic acid (5′) potassium (poly-C), mannan from *Saccharomyces cerevisiae*, cholesterol, CHEMS, 8-hydroxypyrene-1,3,6-trisulfonic acid trisodium salt (HPTS), dexamethasone 21-phosphate disodium salt (DP), Sephadex® G-25 Fine, 3-(4,5-dimethylthiazol- 2-yl)-2,5-diphenyl tetrazolium bromide (MTT), lipopolysaccharides from *Escherichia coli* 0111:B4 (LPS), phorbol 12-myristate

13-acetate (PMA) and 2-mercaptoethanol were from Sigma-Aldrich (MO, USA). Roswell Park Memorial Institute (RPMI) 1640, Dulbecco's Modified Eagle Medium: Nutrient Mixture F-12 (DMEM/F-12), penicillin-streptomycin sulfate, glutamine, sodium pyruvate and trypsin/ethylenediaminetetra acetic acid were from Gibco®, Life Technologies (NY, USA); fetal bovine serum (FBS) was from Internegocios (Cordoba, Argentina). The other reagents were analytic grade from Anedra, Research AG (Buenos Aires, Argentina).

Archaebacteria growth, extraction & characterization of TPAs

Halorubrum tebenquichense archaea, isolated from soil samples of Salina Chica, Península de Valdés and Chubut, Argentina was grown in basal medium supplemented with yeast extract and glucose at 37°C [22]. Biomass was grown in 15-l medium in a 25-l homemade stainless steel bioreactor and harvested 96 h after growth. TPAs were extracted from biomass using the Bligh and Dyer method modified for extreme halophiles [23]. Between 400 and 700 mg TPAs were isolated from each culture batch. The reproducibility of each TPA-extract composition was routinely screened by phosphate content [24] and ESI–MS, as described in [25].

Preparation & characterization of nanoliposomes

Conventional liposomes made of HSPC:cholesterol 9:3 w:w (L), PS-containing liposomes made of soybean phosphatidylcholine:PS 4:1 w:w (L-PS), ARC made of TPA, LpH made of DOPE:CHEMS 7:3 w:w and mixed nanoliposomes made of DOPE:TPA:CHEMS 6.5:0.5:3 w:w (ApH1), 5.6:1.4:3 w:w (ApH2) and 4.2:2.8:3 w:w (ApH3) were prepared by the film hydration method. Briefly, mixtures of lipids were dissolved in chloroform:methanol 1:1 v/v; solvents were rotary evaporated at 40°C until elimination. The lipid films were flushed with N_2 and hydrated with aqueous phase (100 mM Tris-HCl buffer pH 7.4 with 0.9% w:w NaCl-Tris-HCl buffer) up to a final concentration of 10 mg/ml of total lipids (TL). The resultant suspensions were sonicated (1 h with a bath-type sonicator 80 W, 80 kHz) and extruded 21-times through 0.2-µm pore size polycarbonate filters using a manual extruder (Avanti Polar Lipids, AL, USA). The resulting nanoliposomes were sterilized by passage through a 0.22-µm sterile filter, and stored at 4°C.

To prepare RhPE-labeled archaeosomes (RhPE-ARC), RhPE (a fluorescent hydrophobic tracer) was added at 0.5% weight to the TPA.

To prepare HPTS/DPX-containing nanoliposomes (HPTS/DPX-nanoliposomes), lipid films were hydrated with solutions of 35 mM HPTS and 50 mM DPX in Tris-HCl buffer. Free HPTS and DPX were removed from HPTS/DPX-nanoliposomes by gel filtration on Sephadex G-25 using the minicolumn centrifugation technique [26]. Briefly, a 120-µl suspension of nanoliposomes was seeded on top of 3-ml Sephadex G-25 columns. The columns were centrifuged for 5 min at 2000 rpm in a G144D centrifuge (Gelec, Argentina). Fractions of 120 µl were collected eluting with buffer Tris pH 7.4 NaCl 0.9% w/v. The elution profile was determined by quantifying HPTS and phospholipids in each fraction.

To prepare double-labeled nanoliposomes (RhPE and HPTS/DPX), RhPE was added at 0.5% weight to the lipids and lipid films were hydrated with HPTS–DPX solution as stated above.

To prepare DP-containing nanoliposomes (DP-nanoliposomes), lipid films were hydrated with 20 mg/ml of DP in Tris-HCl buffer. Free DP was removed from DP-nanoliposomes by gel filtration as stated above.

Quantification of phospholipid, fluorophores & DP

Phospholipids were quantified by a colorimetric phosphate microassay [24].

RhPE was quantified by spectrofluorometry (λ_{ex} = 561 nm and λ_{em} = 580 nm) upon complete disruption of 1 volume of nanoliposomes in 40 volumes of methanol. The fluorescence intensity (FI) of the sample was compared with a standard curve prepared with RhPE in methanol. The standard curve was linear in the range 0.075–0.5 µg/ml RhPE with a correlation coefficient of 0.999.

HPTS was also quantified by spectrofluorometry (λ_{ex} = 413 nm and λ_{em} = 515 nm) before and after complete disruption of 1 volume of nanoliposomes in 175 volumes of Tris-HCl buffer with Triton X-100 1% w/v. The FI of the sample, calculated as FI with Triton X-100 - FI without disruption, was compared with a standard curve prepared with HPTS–DPX in solution. The standard curve was linear in the range 0.18–12 µM HPTS with a correlation coefficient of 0.996.

DP was quantified by the colorimetric phosphate microassay [24] after extraction of DP from phospholipids using the Bligh and Dyer method [27]. DP was quantified in the aqueous phase while phospholipids were quantified in the chloroform phase.

Size & ζ potential

Size and ζ potential were determined by dynamic light scattering and phase analysis light scattering, respectively, using a nanoZsizer apparatus (Malvern Instruments, Malvern, UK).

Cryo-transmission electron microscopy

Samples were prepared in a controlled environment vitrification system, equilibrated at 22°C and examined in Jeol JEM-1400Plus (JEOL, Japan) instrument, operating at 120 kV. Image collection and measurements were made with Digital Micrograph (Gatan, CA, USA). Images were not processed after acquisition. Sample preparation and data acquisition were performed at the Electron Microscopy Laboratory (LME)/Brazilian Nanotechnology National Laboratory (LNNano).

Cell lines & culture

Immortalized murine Balb/c macrophages J774A.1 (ATCC® TIB-67™), supplied by Dr Erina Petrera (Facultad de Ciencias Exactas y Naturales, Universidad Nacional de Buenos Aires Argentina), were maintained in RMPI 1640 supplemented with 10% FBS, 100 U/ml penicillin, 100 µg/ml streptomycin and 2 mM L-glutamine (complete RMPI medium) in a humidified atmosphere of 5% CO_2 at 37°C.

The human epithelial lung cell line A549 (ATCC® CCL-185™) was bought from Asociación Banco Argentino de Células and the rat alveolar macrophage cell line NR8383 (ATCC CRL-2192™) was supplied by Dr Mirjam Schuchardt (Charité, Universitätmedizin Berlin, Germany). A549 cells and NR8383 cells were maintained in DMEM-F12 supplemented with 10 and 20% of FBS, respectively, 100 U/ml penicillin, 100 µg/ml streptomycin and 2 mM L-glutamine in a humidified atmosphere of 5% CO_2 at 37°C.

The human monocyte cell line THP-1 (ATCC TIB-202™) was supplied by Dr Paula Barrionuevo (Academia Nacional de Medicina, Argentina). The cells were maintained in complete RMPI medium supplemented with 0.05 mM 2-mercaptoethanol and 1 mM sodium piruvate. THP-1, monocytes, were differentiated into macrophages by treatment with 10 ng/ml PMA for 72 h. Then, the medium was replaced by fresh complete RPMI medium and cells were grown for 96 h. The expression of the surface marker CD14 associated with macrophage differentiation was detected by flow cytometry using monoclonal mouse antihuman antibodies IgG1κ CD14-PE (BD Biosciences, CA, USA) [28].

Competitive-binding assay

A competitive-binding assay was performed to assess the involvement of the scavenger receptor class A (SRA) on the endocytic uptake of ARC. The cellular uptake of RhPE-ARC was measured in the presence of different competitors, by flow cytometry, as stated in Supplementary Material.

pH sensitivity in buffers

The pH sensitivity of HPTS/DPX-nanoliposomes was determined by measuring the release of HPTS upon incubation in buffers at different pH. Briefly, 20 µg LT/ml HPTS–DPX–nanoliposomes was incubated for 10 min at 37°C in 10 mM Tris-HCl buffer pH 7.4 and 7 or 10 mM sodium acetate buffer at pH 6.5; 6; 5.5; 5; 4.5 and 4. The FI of HPTS was measured, as stated above, before and after the addition of 1% w/v Triton X-100. The percentage of released HPTS at each pH was calculated as follows: released HPTS (%) = $(FI_{pH} - FI_{pH\ 7.4})/(FI_{Triton\ X\text{-}100} - FI_{pH\ 7.4}) \times 100$, where FI_{pH} was the FI at the indicated pH, $FI_{pH\ 7.4}$ was the FI at pH 7.4 and $FI_{Triton\ X\text{-}100}$ was the FI after the addition of 1% w/v Triton X-100.

Cellular uptake & subcellular pH sensitivity

The uptake and subcellular pH sensitivity of double-labeled RhPE–HPTS/DPX-nanoliposomes were measured by flow cytometry. The uptake of nanoliposomes was followed by the fluorescence of rhodamine, while the fluorescence of HPTS indicated its degree of subcellular dequenching, or pH sensitivity. Briefly, J774A.1, NR8383 and A549 cells were seeded on 24-well culture plates at a density of 1.5×10^5 cells per well and grown for 24 h. Then, cells were incubated with 0.1 mg/ml RhPE–HPTS/DPX-nanoliposomes in a complete medium for different times (0.5, 1 and 3 h) at 37°C. After incubation, the cells were trypsinized, washed with phosphate-buffered saline (PBS) and a total of 1×10^4 cells were analyzed by flow cytometry. For the HPTS, green fluorescence (FL-1) was analyzed, whereas for the RhPE the red fluorescence (FL-3) was analyzed. The fluorescence was further normalized to the HPTS/TL and RhPE/TL ratio of each formulation.

Cell viability

The viability of J774A.1, A549 and differentiated THP-1 cells upon 24-h incubation with empty and DP-loaded nanoliposomes was measured by the MTT assay, as described in the Supplementary Material.

Inhibition of reactive oxygen species generation

The capacity of nanoliposomes to reduce the generation of reactive oxygen species (ROS) by J774.A1 and differentiated THP-1 cells stimulated with LPS was measured using the carboxy-H2DCFDA dye as described in the Supplementary Material.

In vitro anti-inflammatory activity

The *in vitro* anti-inflammatory activity of the nanoliposomes was determined by measuring the release of proinflammatory cytokines by cells stimulated with LPS or PMA. Briefly, J774.A1, A549 and differenti-

ated THP-1 cells were seeded at a density of 2 × 10^5 cells per well onto 24-well plates and grown for 24 h at 37°C. Then cells were coincubated with 1 μg/ml LPS (J774A.1 and THP-1 cells) or 0.1 μg/ml PMA (A549 cells) and empty nanoliposomes (LpH and ApH3 at 50 μg TL/ml), DP-loaded nanoliposomes (DP-LpH and DP-ApH3 at 10 μg DP/ml and 50 μg TL/ml) or DP (10 μg/ml). LPS- or PMA-stimulated and nonstimulated cells without treatments were used as positive and negative controls, respectively. After 24 h of incubation, supernatants were collected and stored at -20°C until analysis.

Mouse TNF-α and IL-6 and human TNF-α, IL-1β and IL-6 levels were measured by enzyme-linked immunosorbent assay (BD OptEIA™, BD Biosciences, CA, USA) following the manufacturer instructions. Absorbance measurements were carried out at 450 nm in a microplate reader.

Stability upon storage

The colloidal stability of nanoliposomes was determined after 3- and 6-month storage at 4°C. Nanoliposomal size and ζ potential before and after storage were determined as stated before.

Stability upon nebulization

The structural stability of nanoliposomes upon nebulization in a vibrating mesh nebulizer (Omron NE-U22, OMRON Healthcare, Japan) was determined in terms of size, polydispersity index and HPTS leakage. Briefly, 2 ml of 50 μg TL/ml HPTS/DPX-nanoliposomes, freshly prepared or after 6 months of storage at 4°C, were nebulized for 5 min. The aerosols were collected in a vessel connected to the nebulizer. Nanoliposomal size, phospholipid and encapsulated HPTS were quantified as stated above, before and after nebulization.

Statistical analysis

Statistical analyses were performed by one-way analysis of variance followed by Dunnet's test using Prisma 4.0 Software (Graph Pad, CA, USA). The p-value of <0.05 was considered statistically significant. *$p < 0.05$; **$p < 0.01$; ***$p < 0.001$; ****$p < 0.0001$; n.s. represents nonsignificant ($p > 0.05$).

Results

Competitive-binding assay

We have previously reported that *in vitro* macrophages take up ARC and archaeolipid-contaning vesicles much more extensively than liposomes prepared with ordinary phospholipids [19,29]. This fact, together with the elevated negative ζ potential of ARC in the order of -40 mV in Tris buffer, suggested that the ARC may be recognized by the endocytic macrophage (Class A) scavenger receptor. To find it out, a competitive binding assay for ARC was performed, according to [30].

It was found that the uptake extent of ARC decreased substantially in 80% after 1 h of incubation with Poly I (Supplementary Figure 2). Neither Poly C, mannose not PS-nanoliposomes inhibited the uptake of ARC by macrophages. These results showed that neither the mannose receptor not the Class B scavenger receptors (responsible for the uptake of PS-nanoliposomes [31] participated, suggested the SRA as the one involved in the uptake of ARC.

Supplementary Figure 3 shows typical cryo-transmission electron microscopy images of ARC, fully made of TPL. Notably, despite being submitted to extrusion, the ARC were seen as mono- or oligolamellar vesicles. Vesicles trapping nanovesicles inside were also observed. Roughly, the mean diameter of ARC was 140 nm, in which the biggest and smaller ARC exhibit diameters of about 500 and 40 nm, respectively.

Formulation of LpH

Once confirmed that SRA were involved in ARC recognition, three new mixed formulations were prepared, starting from a classical pH sensitive formulation that was modified by replacing DOPE by growing amounts of TPA, to obtain the so-called pH-sensitive archaeosomes (ApH). In theory, the new mixed formulations DOPE:TPA:CHEMS would combine pH sensitivity (mediated by acid triggered DOPE collapse to the hexagonal Phase II) with extensive uptake by macrophages and high resistance to physical chemical and enzymatic stress (owed to the TPA). The recovery of TL after extrusion was variable and highest for ApH. The sizes oscillated around 140 and 280 nm, and PDI below 0.46. The ζ potential of ApH was in the order of -40 mV, independently of the content of TPA (Table 1).

Since the inverted cone geometry of DOPE as well and its ratio to CHEMS in LpH is optimal to trigger a phase transition (from lamellar to inverted hexagonal Phase II) at pH between 5 and 4, we assumed the pH sensitivity of the mixed formulations, would be lower than that of the original LpH. We ignored also if the extent of endocytic uptake was proportional to the TPA content of mixed formulations, and if the pH sensitivity was retained after endocytosed. To answer these questions, the pH sensitivity of nanoliposomes was monitored in buffers and their capacity for subcellular release of HPTS was determined.

pH sensitivity of nanoliposomes in buffers

The pH sensitivity of nanoliposomes was tested in buffers by measuring the release of the highly hydrophilic polyanion HPTS (pyranine) from aqueous space, as a function of pH. To that aim, both HPTS and its

Table 1. Structural features of nanoliposomes.

Formulation	Phospholipid concentration (mg/ml ± SD)	Mean diameter (nm ± SD)	PDI	ζ Potential (mV ± SD)	HPTS release pH 4 (%)
LpH	4.1 ± 1	214 ± 14	0.22 ± 0.07	-15.5 ± 1.7	47.4 ± 20.4
ApH1	5.8 ± 0	168 ± 0	0.08 ± 0	-47.9 ± 0	26.6 ± 1.9
ApH2	6.1 ± 1.1	156 ± 14	0.21 ± 0.02	-32.7 ± 7.5	26.3 ± 2.9
ApH3	7.9 ± 0.17	213 ± 20	0.34 ± 0,14	-40.4 ± 4.6	13.8 ± 10.7
ARC	8.7 ± 1.1	144 ± 9	0.34 ± 0.05	-41.3 ± 3.5	2.3 ± 3.5
L	4 ± 0.2	282 ± 53	0.46 ± 0,11	-5.4 ± 1.1	–

Data are expressed as mean ± SD from three independent batches.
HPTS: 8-Hydroxypyrene-1,3,6-trisulfonic acid trisodium salt; PDI: Polydispersity index; SD: Standard deviation.

quencher DPX were loaded to the aqueous space of nanoliposomes at 34.4 and 50 mM respectively. At such concentration ratio, the FI of HPTS is quenched [32]. The nanoliposomes were diluted in buffers of growing acidity, and the FI of HPTS was determined. The HPTS fluorescence increases when dequenched, after released and diluted once destabilized the bilayer, in response to the acidity. The excitation spectra of the HPTS, however, is highly dependent of the pH [33]. For instance, at neutral pH the peak of excitation is at 454 nm, corresponding to an emission peak at 515 nm. At acidic pH, and because of the shift of the excitation at 454 nm, the intensity at 515 nm decreases. In this pH-sensitivity assay, the intensity at λ_{em} 515 nm must follow the HPTS dequenching, not being affected by the pH. To avoid this inconvenience, the excitation was performed at λ_{exc} 413 nm, corresponding to the isosbestic point; in such condition, the intensity of λ_{em} 515 nm is pH independent [34].

Taking LpH as a positive control, the pH sensitivity of ApH1–3 and ARC formulations was determined as a function of the pH. The maximal FI of HPTS was observed for LpH at pH 4, corresponding to a release of 47.4 ± 20% HPTS. Once ordered, the formulations as a function of FI of HPTS (as a synonym of pH sensitivity), the following trend emerged: LpH > ApH1 = ApH2 (26 ± 3% HPTS) > ApH3 (13.8 ± 10.3% HPTS) > ARC (2.0 ± 3.5% HPTS) (Table 1). The ARC – despite not showing significant differences with ApH3 – presented the lowest release of HPTS at pH4, and was thus classified as non-pH-sensitive formulation. These results showed an inverse relationship between the TPA content and pH-sensitivity for the mixed formulations DOPE: TPA: CHEMS.

Subcellular release of HPTS from nanoliposomes

The assessment of nanoliposomal pH sensitivity in buffers was complemented by determining the subcellular pH sensitivity on murine macrophages J774A.1, rat alveolar macrophages NR8383 cells and the human epithelial lung cells A549. To that aim, the nanoliposomes were doubly labeled with HPTS-DPX in the aqueous space and RhPE (that at <1% mol does not affect the pH sensitivity [35] in the bilayer. The FI of RhPE indicated the extent of endocytic uptake whereas the FI of HPTS accounted for its cytoplasmic release. The RhPE/lipids ratio was similar in all formulations; the HPTS/lipids ratio was highest for ApH2 and ApH3 (52–56), intermediate for LpH and ARC (26–20) and lowest for L (Supplementary Table 1). The ratio value for each sample was used to normalize the readings on flow cytometry.

Since ApH1 and ApH2 showed undistinguishable response to acidity, in this assay only ApH2 and ApH3 were tested. Besides, a non-pH-sensitive and very rigid conventional formulation of liposomes made of HSPC: cholesterol, 9:3 w:w (L) was included. The uptake was determined on three cell lines, two of them (A549 and NR8383) not expressing SRA (data not shown).

The extent of uptake by the three cell types – measured by the FI of RhPE – varied with the nanoliposome composition (Figure 1), and was proportional to the TPA content; the following trend was found: uptake of ARC (100% TPA) > ApH3 > ApH2 > LpH > L. The absolute amount of uptake was highest in J774A.1, resulting between 10- and 12-folds higher than in NR8383 and A549 cells, as judged by the normalized FI of RhPE.

The subcellular release of HPTS, on the other hand, was highest for ApH3 in the three cell types. In J774A.1 cells, the FI of HPTS followed the trend: ApH3 > LpH = ApH2 > ARC > L. In NR8383 and A549 cells, the observed trend was similar: ApH3 > LpH = ARC = ApH2 > L. No cellular uptake or HPTS release was found for L.

DP in nanoliposomes

Since it provided the highest cytoplasmic fluorescence of HPTS, ApH3 was the mixed formulation chosen to be loaded with DP (DP-ApH3). DP-L (non-pH-sensitive/low uptake), DP-ARC (non-pH-sensitive/high uptake) and DP-LpH (pH-sensitive/intermediate uptake) were also prepared.

The DP/TL ratio for each formulation is shown in Supplementary Table 2. Most of DP was not encapsulated; nonetheless, the free DP was removed by the gel filtration column. Besides of dissolving in the aqueous space, DP also partitioned in the nanoliposome bilayer. Different from HPTS (a negatively charged dye that does not interact with anionic bilayers at any pH), DP partitions according to the pH and the structural nature of the bilayers, to be highest at acid pH and on high entropic disordered bilayers in liquid crystalline state [36,37]. The DP/LT ratios suggested the partition of DP was minimal on the rigid HSPC:cholesterol bilayer of L, to increase for ARC and ApH3. These last bilayers exhibit a surface tension lower than of ordinary phospholipids, arising from the bulky and fluid polyisoprenoid due to the abnormally large limiting occupied area of the archaeal lipids (nearly 110–125 $Å^2$ per archaeolipid molecule vs 57–60 $Å^2$ for DMPC) [38]. The highest partition corresponded to LpH. The high standard deviation in DP quantification would arise from the variability owed to the separation of DP from lipids by the Bligh and Dyer method.

Cell viability

In Supplementary Figure 4 the viability of A549, J774A.1 and THP-1 cells after incubation with void and DP-containing nanoliposomes as determined by MTT is shown. It was found that the viability of A549 cells did not significantly decrease for any sample between 7 and 220 μg TL/ml and 1.5 and 50 μg DP/ml after 24 h. On the other hand, the viability of J774A.1 cells decreased at the highest TL concentrations of ARC and ApH3, void or DP-containing. The viability of THP-1 cells decreased only for DP-ApH3 at highest TL. Free DP did not affect the viability on any cell line in the tested concentrations.

Taken together, these results showed that phagocytic cells J774A.1 and THP-1, were more sensitive than A549 cells to the highest concentrations of DP-ApH3 and DP-ARC. It can be speculated that above 220 μg TL /ml, the endocytic uptake of TPA containing nanoliposomes would cause a lipid overdose toxic for J774A.1 cells. The THP-1 cells, on the other hand, would be more sensitive to a cytoplasmic overdose of DP, released from DP-ApH3.

Inhibition of ROS generation

In Supplementary Figure 5, the subcellular ROS – measured by the fluorescence of oxidized DCFDA – on J774A.1 and THP-1 cells after incubating LPS with void and DP-containing nanoliposomes (10 μg DP and 50 μg TL/ml) is shown. On J774A.1 cells, DP-ApH3 decreased the ROS levels below those of free DP. The effect of DP-LpH was comparable to the induced by free DP. On THP-1 cells, a similar but less pronounced trend was observed for DP-ApH3 and DP-LpH.

The results suggest as well that besides being more intense at the same dose, the anti-inflammatory activity of DP- ApH3 occurred at similar or higher speed than that of free DP.

Anti-inflammatory effect of nanoliposomes on cells stimulated with LPS or PMA

The effect of nanoliposomes on proinflammatory cytokines levels was determined after cell incubation with 1 μg/ml LPS or 0.1 μg/ml PMA in culture media for 24 h.

In Figure 2A & B the levels of IL-6 and TNF-α induced on J774A1 cells are shown. While free DP slightly reduced the IL-6 titer, DP-ApH3 completely suppressed it. While DP-LpH had no anti-inflammatory effect, a slight decrease in IL-6 was noticed for void ApH3. Accordingly, while free DP slightly decreased the TNF-α levels, DP-ApH3 was again the main suppressor of TNF-α. The remainder formulations did not significantly affect the TNF-α levels.

In Figure 2C–E the levels of IL-6, TNF-α and IL-1β induced on differentiated THP-1 cells are shown. Again, while free DP slightly reduced the IL-6, TNF-α and IL-1β titers, DP-ApH3 was the formulation inducing the more pronounced decrease in the three cytokines levels. In this cell line, all the nanoliposomes had a slight anti-inflammatory effect.

The lung epithelial cells A549 cell, stimulated with PMA showed a completely different pattern of IL-6 levels. Figure 2F shows that free DP and by void or DP-containing LpH caused a similar reduction on IL-6 titers.

Stability of nanoliposomes upon storage & after nebulization stress

The size and HPTS content of freshly prepared and stored for 6 months at 4°C HPTS-DPX-nanoliposomes were determined before and after nebulization. We observed that freshly prepared ApH3 and LpH retained size, PDI and HPTS/TL ratio (indicative of HPTS retained in nanoliposomes). We also detected that 75% of ApH and 50% of LpH lipids were recovered after nebulization (Table 2, Supplementary Figures 6 & 7).

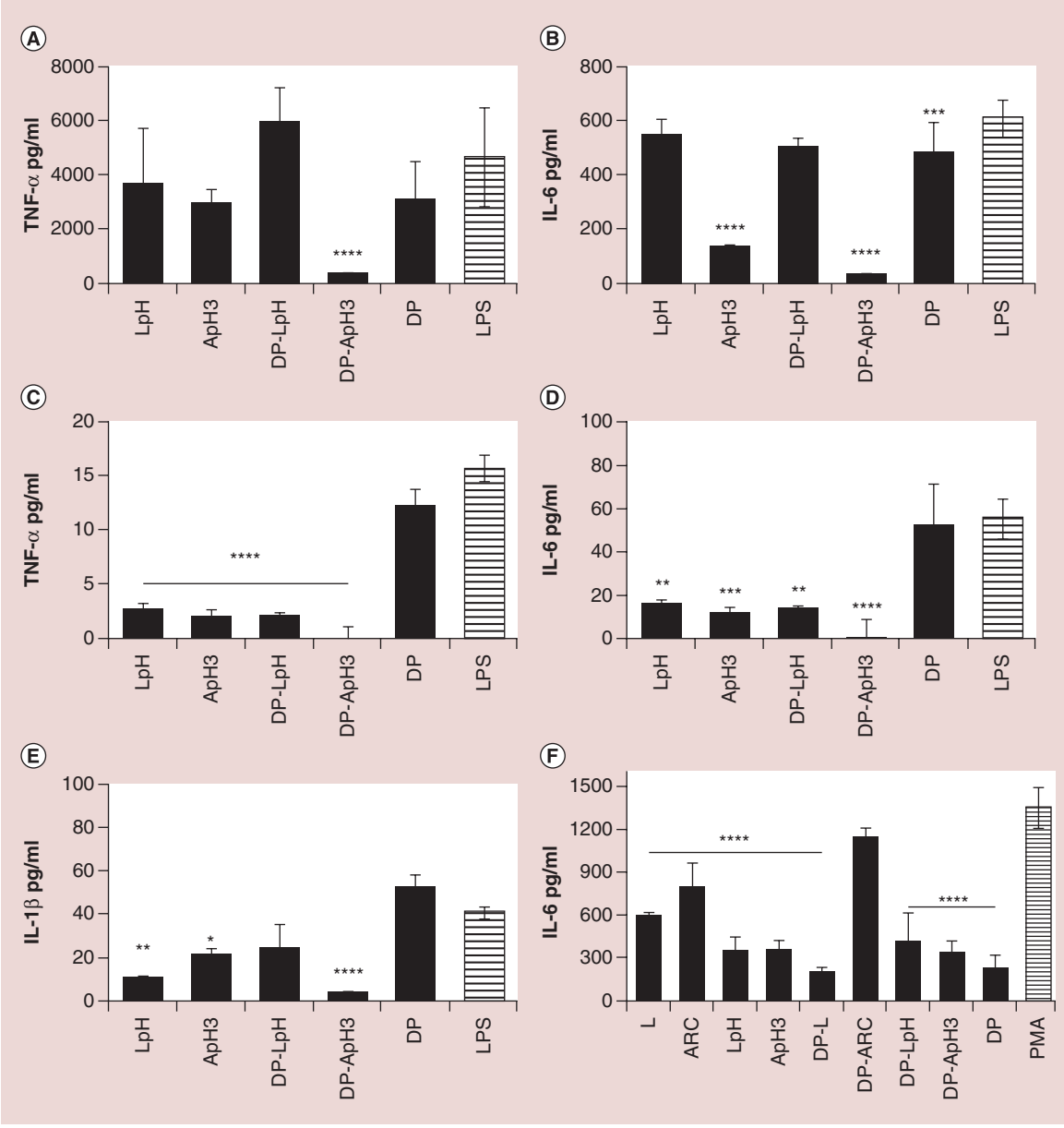

Figure 2. *In vitro* anti-inflammatory activity. Proinflammatory cytokines released by J774A.1 cells **(A & B)**, differentiated THP-1 cells **(C–E)** and A549 cell **(F)** where measured upon 24 h of coincubation of nanoliposomes with 1 μg/ml LPS for macrophages or with 0.1 μg/ml PMA for A549 cells. Values are expressed as means ± SD (n = 2 batches).
LPS: Lipopolysaccharides from *Escherichia coli* 0111:B4; PMA: Phorbol 12-myristate 13-acetate; SD: Standard deviation.

After 6 months of storage, however, the size and PDI of LpH increased from 150 to 300 nm, and from 0.1 to 0.4, respectively (Supplementary Figure 6). After nebulization, the HPTS loss was complete, and the lipid recovery, despite of being negligible showed nanoliposomes of increased size and PDI (Table 2, Supplementary Figure 7). In contrast, after 6 months of storage, ApH3 retained size and PDI (100–150 nm and 0.1–0.2, respectively). After nebulization the size, PDI and HPTS/TL ratio of ApH3 remained the same as freshly prepared formulations, being recovered again 75% of the ApH lipids.

Discussion

We present here the structural characterization and anti-inflammatory activity screening of mixed nanoliposomes DOPE:TPA:CHEMS (ApH), loaded with the model corticosteroid DP. We reasoned that the introduction of ligands for endocytic receptors

Table 2. Phospholipids and encapsulated 8-hydroxypyrene-1,3,6-trisulfonic acid trisodium salt quantification before and after nebulization.

Formulation	Before NB		After NB					
	Encapsulated HPTS (μg/ml ± SD)	TL (μg/ml ± SD)	Encapsulated HPTS (μg/ml ± SD)	Free HPTS (μg/ml ± SD)	TL (μg/ml ± SD)	Encapsulated HPTS (%)	Free HPTS (%)	TL (%)
ApH3 (0)	3.6 ± 0.1	50 ± 3	2.7 ± 0.2	0.7 ± 0.02	36.6 ± 1.4	75 ± 4	19.6 ± 0.1	74 ± 2
LpH (0)	4.6 ± 0.1	36.8 ± 1.8	2.4 ± 0.02	1.9 ± 0.1	20 ± 1	53 ± 1	41.3 ± 1.2	54 ± 0
ApH3 (6)	7.4 ± 0.3	50 ± 2.1	5.4 ± 0.2	0.9 ± 0.1	33.3 ± 0.6	73 ± 4	11.5 ± 1.2	67 ± 1
LpH (6)	3.6 ± 0.2	44.2 ± 1.1	0	3.5 ± 0.2	<3.4	0	98.4 ± 2.8	<7.7

Freshly prepared nanoliposomes, (6) Nanoliposomes after 6 months storage at 4°C.
HPTS: 8-Hydroxypyrene-1,3,6-trisulfonic acid trisodium salt; NB: Nebulization; SD: Standard deviation; TL: Total lipid.

involved in massive uptake of particulate material, would increase the efficiency of LpH for cytoplasmic delivery of DP. Because of their high uptake rate, the hemoglobin scavenger receptor CD163 and the types I and II class A scavenger receptors (SRA) have started gathering considerable interest as receptors for targeted nanoparticles-based therapies [39,40]. Particularly the SRA are endocytic receptors specialized in clearance of cells, molecules and particles, involved in host defence mostly expressed in rat and human macrophages. SRA are membrane bound proteins acting as pattern recognition receptors to clear bacterial endotoxin from the blood and to aid in the ingestion of unopsonized Gram-positive lipoteichoic acid and Gram-negative bacteria lipid-A moiety of lipopolysaccharide (LPS). SRA also bind modified forms of LDL including acetyladed LDL, oxidized LDL malondialdehyde-LDL, maleylated LDL and other polyanionic ligands [41–45].

The first step of our experimental approach consisted on assessing the effect of replacing DOPE by TPA on nanoliposome's pH sensitivity, on buffers of increased acidity. Once classified according to their pH sensitivity, the efficiency of each nanoliposome for subcellular delivery of HPTS was determined. We found that despite its low pH sensitivity (barely exceeding that of the non-pH-sensitive ARC), ApH3 provided the maximal subcellular delivery of HPTS, once endocytosed by the three cell lines. In this assay, the subcellular delivery of HPTS was remarkably driven by two factors: the intrinsic mechanism of nanoliposomes pH sensitivity and the extent of its endocytic uptake. We found that the huge content of TPA in ApH3, responsible for its low pH sensitivity in buffers, was also responsible for its extensive endocytic uptake (between two- and threefolds higher than of LpH at 3 h). The balance in favor of the extensive uptake, resulted in maximal subcellular delivery of HPTS in the three cell lines. The low ph sensitivity of ApH3, where DOPE is partly replaced by TPA may be caused by an impaired transition to the hexagonal Phase II of DOPE. At 37 C DOPE bilayers in alkaline media (and DOPE:CHEMS bilayers at neutral pH) are in the liquid crystalline phase [46], the same as TPA bilayers. The TPA bilayers however, though highly entropic, display a relatively low permeability and reduced lateral diffusion [38]. If well TPA and DOPE can form fully mixed homogeneous system [47], the presence of TPA in the bilayer may difficult the spatial assemblage of DOPE in a new hexagonal phase.

The extent of endocytic uptake of ApH3 in J774A.1 cells – the only cell line expressing SRA – was between 12- and 10-folds higher than in A549 and NR8383 cells, respectively. In A549 and NR8383 cells, however, the endocytoses of nanoliposomes were – similar to J774A.1 cells – proportional to its TPA content. The TPA is a natural extract consisting in phosphatidylglycerophosphate methyl ester, sulfated diglycosyl diphytanylglycerol diether (SDGD), SDGD-5PA, phosphatidylglycerol, and bisphosphatidyl glycerol) [22]. The PGP-ME is a major component of the TPA and was responsible for the extensive uptake by J774A.1 cells [UNPUBLISHED DATA]. A potential explanation of the endocytoses proportional to the TPA content in A549 cells is that sugars such as SDGD and SDGD-5PA in TPA may also be recognized by receptors for advanced glycation products, that A549 cells utilize instead of SRA [48].

The effect of the DP-LpH on ROS generation, as an early response previous to inflammation, was additionally tested. In macrophages for instance, LPS quickly stimulates NADPH oxidase-derived ROS before inducing, 3 h later the proinflammatory cytokines IL-1β and TNFα [49]. The effect of DP-LpH on ROS generation, hence, would account for the efficiency of the cytoplasmic delivery of DP upon endocytoses, compared with diffusion of free DP. As expected, we found that DP-ApH3 was the more effective at reducing the levels of ROS in J774A1 and in THP cells.

In a second step, we found that the formulation DP-ApH3, despite its low DP/lipid ratio, induced the highest decrease of IL-6, TNF-α and IL-1β titers on J774A.1 and THP-1 cells stimulated with LPS. Surprisingly, void and DL-nanoliposomes exhibited anti-inflammatory activity on THP1 cells. This fact could be owed to LPS (of 10–14 μg LPS/ml critical micellar concentration) monomers that may insert in the nanoliposomal bilayer, thus decreasing its availability to stimulate the TLR4 [50].

Accordingly, DP-LpH – the formulation that provided the lowest cytoplasmic delivery of HPTS – was also the less effective to reduce the levels of proinflammatory cytokines. These results suggest that the access of hydrosoluble drugs to the cytoplasmic receptor – and thus the drug efficacy – may be increased by means of a pH-sensitive carrier of high endocytic uptake such as the SRA.

The A549 cells on the other hand, are closely similar to the type II alveolar epithelial cells in that they also synthesize disaturated phosphatidylcholines and secrete surfactant. Type II alveolar epithelial cells cover approximately 4% of the mammalian alveolar surface but constitute 15% of all lung cells and may act as sentinels in the defense against infection [51]. In asthma therapy, alveolar epithelial cells are one of the most important targets for IC, because these cells are involved in the secretion of many proinflammatory proteins [52]. Different to J774A.1 and THP-1 cells, however, we found that in A549 the anti-inflammatory activity of DP was identical to that of LpH, carrying DP or not. Curiously, CHEMS lacking nanoliposomes such as L or ARC decreased the IL-6 titers in a much lower extent. We can speculate that in A549 cells, CHEMS in LpH may compete with intermediates of the same signaling route used by PMA to induce IL-6. CHEMS is metabolically unaltered by cells, and could constitutively activate signal transduction processes. Similar to bulky polyunsaturated fatty acids CHEMS is described to exhibit antiproliferative and apoptotic activities; to activate protein kinase C isoenzymes, and to increase the local intracellular Ca^{+2} concentration adjacent to the membrane, due to generation of a negative electrostatic potential. The accurate interpretation of these results needs of substantial experimental evidence that is out of the scope of this work. Overall, we observed that in A549 cells the extent of endocytic uptake of all nanoliposomes was low but probably dependent on the sugar fraction in TPA. The results suggest as well that the extent of subcellular delivery of nanoliposomal HPTS is not related to a high anti-inflammatory activity of nanoliposomal DP, unless its endocytoses was mediated by SRA, a receptor absent in A549 cells.

Aiming for selective targeting, the surface of nanocarriers has been covalently linked to a wide structural variety of ligands, by chemical processes of relative complexity, most of them expensive. Not always such elaborated handling meets the expected therapeutic success. The high cost/benefit of the targeted approaches difficult their industrial implementation [53]. In order to reduce their high attrition rates, it is essential, thus, to count on methods to prepare targeted nanoliposomes as simple and cheap as possible.

Previously, we have reported that TPA and phospholipids can be combined in different ratios simply by mixing organic solutions, to render new homogeneous liposomal bilayers [48]. In this work, we found that the reduced pH sensitivity following the replacement of growing amounts of DOPE by TPA on original DOPE:CHEMS matrices, was counterbalanced by making the ApH3 recognizable by SR-AI/II expressed both on J774A.1 [30] and in THP-1 [54], a fact ending on the highest subcellular delivery of HPTS, and presumably of the DP. Similar to J774A1 and THP-1, lung macrophages express MARCO (macrophage receptor with collagenous structure) and SR-AI/II, to promote the uptake and clearance of inhaled particles and bacteria [55]. The cell-targeted ApH3 were prepared by simple lipid mixing, neither by covalent binding nor by insertion of ligands in preformed vesicles. As previously mentioned, the multistep procedures not always allow for a stoichiometric control of ligands amount, complicating the quality assurance and increasing the final cost of targeted formulations [56].

On the other hand, the effective deposition of inhaled liposomes in the distal parts of the lungs (respirable fraction) is as a function of the nebulizer and compressor. It is the aerosol droplet size, not the liposome size, which determines the site of deposition [57]. In this framework, maintaining the critical physical properties of liposomes after nebulization holds the key for a successful liposomal product [58]. The most suitable method for nebulization of liposomal formulations is the vibrating-mesh techno [59], because of its ability to deliver higher density aerosols with greater efficiency than jet nebulizers, thus leading to a shorter treatment time. Vibrating-mesh nebulizers also hold a reduced potential to disrupt liposomes, because there is no re-exposure of fluid to the aerosol generation process, although a greater loss of encapsulated drug with increasing vesicle size has been reported for mesh nebulizers. The energetics of the vibrating mesh affects liposomes upstream of the mesh in addition to those that pass through the mesh. As a result, these nebulizers are responsible for high release rate of encapsulated cargoes [59]. Liposomal size and lamellarity, encapsulation efficiency and *in vitro* release rate should be main-

tained after aerosolization to provide assurance that the *in vivo* release profile will be consistent for every patient. Small -sized unilamellar liposomes with mean size typically in the range of approximately 30–150 nm [14] are less susceptible to shear and more robust to the nebulization process [60,61]. Rigid bilayers (having 30% cholesterol or lipids with high phase transition temperatures (e.g., above room temperature)), are needed to increase pulmonary drug retention [61]. In a recent work, flexible liposomes of low Young's modulus were prepared in an attempt to improve their resistance against shear stress. The strategy failed, rendering a complete drug lost during nebulization [62]. In our case, including TPA in DOPE:CHEMS nanoliposomes had consequences beyond that of changing the carrier pharmacodynamics. The intrinsic chemical structure of the archaeolipids significantly increased the endurance of nanoliposomes to the storage and to the nebulization. When nebulized in a vibrating mesh device after 6-month storage, there was a high recovery of ApH3 nanoliposomes fully retaining original HPTS, whereas the recovery of LpH was almost negligible, besides of completely losing its original HPTS. These results suggested that the physical stability of TPA-containing nanoliposomes to nebulization may well manage without including cholesterol or expensive hydrogenated lipids of high phase transition temperature in the nanoliposome bilayer.

Taken together, these results show for the first time that by simple mixing archaeolipids and ordinary phospholipids, nanoliposomes of higher colloidal endurance than liposomes, exposing specific ligands, were obtained. The inhaled targeted liposomes are still an emergent technology [63], and in such scenario, our results suggest that *in vivo* the inhaled pH-sensitive ARC may enhance the activity of corticosteroids.

Supplementary data

To view the supplementary data that accompany this paper please visit the journal website at: www.futuremedicine.com/doi/full/10.2217/nnm-2016-0165

Acknowledgements

The authors would like to thank Dr de Farias and Dr Portugal from the Electron Microscopy Laboratory, Brazilian Nanotechnology National Laboratory, for sample preparation and data acquisition of Cryo-TEM images.

Financial & competing interests disclosure

The authors have no relevant affiliations or financial in-

Executive summary

Background

- Inhaled carriers for site-specific drug delivery may yet evolve toward more sophisticated nanoparticles displaying new functionalities, compatible with their industrial manufacture. It would be desirable, for instance, to count on carriers enabling the drugs to be delivered to a specific subcellular site (tertiary targeting).
- The inclusion of total polar archaeolipids (TPAs) in pH-sensitive nanoliposomes (LpH) may result on nanoliposomes exhibiting new pharmacodynamic properties. The TPA may also increase the mechanical stability of the bilayer during nebulization, which is responsible for the loss of the liposomal drug. In order to reduce their high attrition rates, it is essential to count on methods to prepare targeted nanoliposomes as simple and cheap as possible.

Results & discussion

- The formulation dexamethasone phosphate in pH-sensitive archaeosomes (ApH3 made of dioleylphosphatidylethanolamine: TPA: cholesteryl hemisuccinate), induced the highest decrease of IL-6, TNF-α and IL-1β titers on J774A.1 y THP-1 cells stimulated with lipopolysaccharides from *Escherichia coli* 0111:B4.
- Accordingly, dexamethasone phosphate in LpH made of dioleylphosphatidylethanolamine:cholesteryl hemisuccinate – the formulation that provided the lowest cytoplasmic delivery of the fluorescent dye HPTS (8-hydroxypyrene-1,3,6-trisulfonic acid trisodium salt) – was also the less effective to reduce the levels of proinflammatory cytokines.
- When nebulized in a vibrating mesh device after 6-month storage, there was a high recovery of ApH3 nanoliposomes fully retaining its original HPTS, whereas the recovery of LpH was almost negligible, besides of completely losing its original HPTS.

Conclusion

- The access of hydrosoluble drugs to the cytoplasmic receptor – and thus the drug efficacy – may be increased by means of a pH-sensitive carrier of high endocytic uptake such as the scavenger receptor class A.
- It can also be stated that the physical stability of TPA-containing nanoliposomes to nebulization may well manage without including cholesterol or expensive hydrogenated lipids of high phase transition temperature in the nanoliposome bilayer.

volvement with any organization or entity with a financial interest in or financial conflict with the subject matter or materials discussed in the manuscript. This includes employment, consultancies, honoraria, stock ownership or options, expert testimony, grants or patents received or pending, or royalties.

No writing assistance was utilized in the production of this manuscript.

References

Papers of special note have been highlighted as: • of interest; •• of considerable interest

1 Ricciardolo FL, Blasi F, Centanni S, Rogliani P. Therapeutic novelties of inhaled corticosteroids and bronchodilators in asthma. *Pulm. Pharmacol. Ther.* 33 1–10 (2015).

•• **Complete updated overview on pharmacological features of available conventional inhaled corticosteroids and bronchodilators with a focus on fluticasone propionate/formoterol fumarate combination.**

2 Bathoorn E, Kerstjens H, Postma D, Timens W, Macnee W. Airways inflammation and treatment during acute exacerbations of COPD. *Int. J. Chron. Obstruct. Pulmon. Dis.* 3(2), 217 (2008).

3 Gaude G, Nadagouda S. Nebulized corticosteroids in the management of acute exacerbation of COPD. *Lung India* 27(4), 230 (2010).

4 Kelly HW. Comparison of inhaled corticosteroids: an update. *Ann. Pharmacother.* 43(3), 519–527 (2009).

5 Stanbury RM, Graham EM. Systemic corticosteroid therapy – side effects and their management. *Br. J. Ophthalmol.* 82, 704–708 (1998).

6 Kuzmov A, Minko T. Nanotechnology approaches for inhalation treatment of lung diseases. *J. Control. Release* 219, 500–518 (2015).

7 Paranjpe M, Müller-Goymann CC. Nanoparticle-mediated pulmonary drug delivery: a review. *Int. J. Mol. Sci.* 15(4), 5852–5873 (2014).

•• **Concise review focused on the current status of different colloidal systems available for the treatment of various lung disorders along with their characterization. Includes data on different *in vitro*, *ex vivo* and *in vivo* cell models developed for the testing of these systems with studies involving cell culture analysis.**

8 Cipolla D, Redelmeier T, Eastman S, Bruinenberg P, Gonda I. Liposomes, niosomes and proniosomes-a critical update of their (commercial) development as inhaled products. In: *Respiratory Drug Delivery Europe.* Dalby RN, Byron PR, Peart J, Suman JD, Farr SJ, Young PM (Eds). Davis Healthcare Int'l Publishing, IL, USA, 41–54 (2011).

9 Sercombe L, Veerati T, Moheimani F, Wu SY, Sood AK, Hua S. Advances and challenges of liposome assisted drug delivery. *Front. Pharmacol.* 6, 286 (2015).

•• **A review highlighting the advances in liposome-assisted drug delivery, biological challenges remaining, current clinical and experimental use of liposomes for biomedical applications. Includes an overview of translational obstacles of liposomal technology.**

10 Chang HI, Yeh MK. Clinical development of liposome-based drugs: formulation, characterization, and therapeutic efficacy. *Int. J. Nanomedicine* 7 49–60 (2012).

11 Allen TM, Cullis PR. Liposomal drug delivery systems: from concept to clinical applications. *Adv. Drug Deliv. Rev.* 65(1), 36–48 (2013).

12 Serisier DJ, Bilton D, De Soyza AG *et al*. Inhaled, dual release liposomal ciprofloxacin in non-cystic fibrosis bronchiectasis (ORBIT-2): a randomised, double-blind, placebo-controlled trial. *Thorax* 68(9), 812–817 (2013).

13 Cipolla D, Blanchard J, Gonda I. Development of liposomal ciprofloxacin to treat lung infections. *Pharmaceutics* 8(1), 6 (2016).

•• **An updated landscape on the performance of two liposomal ciprofloxacin formulations (Lipoquin® and Pulmaquin®) in development by Aradigm Corporation.**

14 Cipolla D, Gonda I, Chan HK. Liposomal formulations for inhalation. *Ther. Deliv.* 4(8), 1047–1072 (2013).

•• **A seminal review highlighting the safety of inhaled liposomes and summarizing the clinical experience with liposomal formulations for pulmonary application.**

15 Rajendran L, Knölker HJ, Simons K. Subcellular targeting strategies for drug design and delivery. *Nat. Rev. Drug Discovery* 9(1), 29–42 (2010).

16 Morilla M, Romero E. Liposomal pH-sensitive nanomedicines in preclinical development. In: *Bionanotechnology II: A Global Prospect.* Reisner D (Ed.). CRC Press, Boca Raton, FL, 383–413 (2012).

17 Paliwal SR, Paliwal R, Vyas SP. A review of mechanistic insight and application of pH-sensitive liposomes in drug delivery. *Drug Deliv.* 22(3), 231–242 (2015).

18 Corcelli A, Lobasso S. Characterization of lipids of halophilic archaea. In: *Methods in Microbiology – Extremophiles (Volume 35)*. Rainey AF, Oren A (Eds). Elsevier, Amsterdam, The Netherlands, 585–613 (2006).

19 Perez AP, Casasco A, Schilrreff P *et al*. Enhanced photodynamic leishmanicidal activity of hydrophobic zinc phthalocyanine within archaeolipids containing liposomes. *Int. J. Nanomedicine* 9 3335–3345 (2014).

20 Verstraelen S, Bloemen K, Nelissen I, Witters H, Schoeters G, Van Den Heuvel R. Cell types involved in allergic asthma and their use in *in vitro* models to assess respiratory sensitization. *Toxicol. In Vitro* 22(6), 1419–1431 (2008).

21 Morilla MJ, Montanari J, Frank F *et al*. Etanidazole in pH-sensitive liposomes: design, characterization and *in vitro*/*in vivo* anti-*Trypanosoma cruzi* activity. *J. Control. Release* 103(3), 599–607 (2005).

22 Gonzalez RO, Higa LH, Cutrullis RA *et al*. Archaeosomes made of *Halorubrum tebenquichense* total polar lipids: a new source of adjuvancy. *BMC Biotechnol.* 9(1), 71 (2009).

23 Kates M, Kushwaha SC. Isoprenoids and polar lipids of extreme halophiles. In: *Archaea: A Laboratory Manual, Halophiles*. Dassarma S (Ed.). Cold Spring Harbor Laboratory Press, NY, USA, 35–54 (1995).

24 Bötcher CJF, Van Gent CM, Pries C. A rapid and sensitive sub-micro phosphorus determination. *Anal. Chim. Acta.* 24, 203–204 (1961).

25 Higa LH, Schilrreff P, Perez AP *et al*. Ultradeformable archaeosomes as new topical adjuvants. *Nanomedicine* 8(8), 1319–1328 (2012).

26 Fry DW, White JC, Goldman ID. Rapid separation of low molecular weight solutes from liposomes without dilution. *Anal. Biochem.* 90(2), 809–815 (1978).

27 Bligh EG, Dyer WJ. A rapid method of total lipid extraction and purification. *Can. J. Biochem. Phys.* 37(8), 911–917 (1959).

28 Park EK, Jung HS, Yang HI, Yoo MC, Kim C, Kim KS. Optimized THP-1 differentiation is required for the detection of responses to weak stimuli. *Inflamm. Res.* 7(1), 45–50 (2007).

29 Higa LH, Arnal L, Vermeulen M *et al*. Ultradeformable archaeosomes for needle free nanovaccination with *Leishmania braziliensis* antigens. *PloS One* 11(3), e0150185 (2016).

30 Wang H, Wu L, Reinhard BM. Scavenger receptor mediated endocytosis of silver nanoparticles into J774A.1 macrophages is heterogeneous. *ACS Nano* 6(8), 7122–7132 (2012).

31 Kawasaki Y, Nakagawa A, Nagaosa K, Shiratsuchi A, Nakanishi Y. Phosphatidylserine binding of class B scavenger receptor type I, a phagocytosis receptor of testicular sertoli cells. *J. Biol. Chem.* 277(30), 27559–27566 (2002).

32 Van Bambeke F, Kerkhofs A, Schanck A *et al*. Biophysical studies and intracellular destabilization of pH-sensitive liposomes. *Lipids* 35(2), 213–223 (2000).

33 Clement NR, Gould JM. Pyranine (8-hydroxy-1, 3, 6-pyrenetrisulfonate) as a probe of internal aqueous hydrogen ion concentration in phospholipid vesicles. *Biochemistry* 20(6), 1534–1538 (1981).

34 Straubinger RM, Papahadjopoulos D, Hong K. Endocytosis and intracellular fate of liposomes using pyranine as a probe. *Biochemistry* 29(20), 4929–4939 (1990).

35 Slepushkin VA, Simões S, Dazin P *et al*. Sterically stabilized pH-sensitive liposomes intracellular delivery of aqueous contents and prolonged circulation *in vivo*. *J. Biol. Chem.* 272(4), 2382–2388 (1997).

36 Marqusee J, Dill KA. Solute partitioning into chain molecule interphases: monolayers, bilayer membranes, and micelles. *J. Chem. Phys.* 85(1), 434–444 (1986).

37 Modi S, Anderson BD. Bilayer composition, temperature, speciation effects and the role of bilayer chain ordering on partitioning of dexamethasone and its 21-phosphate. *Pharm. Res.* 30(12), 3154–3169 (2013).

38 Kitano T, Onoue T, Yamauchi K. Archaeal lipids forming a low energy-surface on air–water interface. *Chem. Phys. Lipids* 126(2), 225–232 (2003).

39 Jain NK, Mishra V, Mehra NK. Targeted drug delivery to macrophages. *Expert Opin. Drug Deliv.* 10(3), 353–367 (2013).

40 Graversen JH, Svendsen P, Dagnæs-Hansen F *et al*. Targeting the hemoglobin scavenger receptor CD163 in macrophages highly increases the anti-inflammatory potency of dexamethasone. *Mol. Ther.* 20(8), 1550–1558 (2012).

41 Brown JM, Swindle EJ, Kushnir-Sukhov NM, Holian A, Metcalfe DD. Silica-directed mast cell activation is enhanced by scavenger receptors. *Am. J. Respir. Cell Mol. Biol.* 36(1), 43–52 (2007).

42 Loboda A, Jazwa A, Jozkowicz A, Molema G, Dulak J. Angiogenic transcriptome of human microvascular endothelial cells: effect of hypoxia, modulation by atorvastatin. *Vascul. Pharmacol.* 44(4), 206–214 (2006).

43 Plüddemann A, Neyen C, Gordon S. Macrophage scavenger receptors and host-derived ligands. *Methods* 43(3), 207–217 (2007).

44 Pierini LM. Uptake of serum-opsonized *Francisella tularensis* by macrophages can be mediated by class A scavenger receptors. *Cell. Microbiol.* 8(8), 1361–1370 (2006).

45 Mukhopadhyay S, Gordon S. The role of scavenger receptors in pathogen recognition and innate immunity. *Immunobiology* 209(1–2), 39–49 (2004).

46 Ellens H, Bentz J, Szoka FC. Destabilization of phosphatidylethanolamine liposomes at the hexagonal phase transition temperature. *Biochemistry* 25 (2), 285–294 (1986).

47 Carrer DC, Higa LH, Tesoriero MVD, Morilla MJ, Roncaglia DI, Romero EL. Structural features of ultradeformable archaeosomes for topical delivery of ovalbumin. *Colloids Surf. B.* 121 281–289 (2014).

48 Nakano N, Fukuhara-Takaki K, Jono T *et al*. Association of advanced glycation end products with A549 cells, a human pulmonary epithelial cell line, is mediated by a receptor distinct from the scavenger receptor family and RAGE. *J. Biochem.* 139(5), 821–829 (2006).

49 Hsu HY, Wen MH. Lipopolysaccharide-mediated reactive oxygen species and signal transduction in the regulation of interleukin-1 gene expression. *J. Biol. Chem.* 277(25), 22131–22139 (2002).

50 Alam JM, Yamazaki M. Spontaneous insertion of lipopolysaccharide into lipid membranes from aqueous solution. *Chem. Phys. Lipids* 164(2), 166–174 (2011).

51 Chuquimia OD, Petursdottir DH, Rahman MJ, Hartl K, Singh M, Fernández C. The role of alveolar epithelial cells in initiating and shaping pulmonary immune responses: communication between innate and adaptive immune systems. *PLoS One* 7(2), e32125 (2012).

52 Nonaka T, Nave R, Mccracken N, Kawashimo A, Katsuura Y. Ciclesonide uptake and metabolism in human alveolar type II epithelial cells (A549). *BMC Pharmacol.* 7(1), 12 (2007).

53 Kraft JC, Freeling JP, Wang Z, Ho RJ. Emerging research and clinical development trends of liposome and lipid nanoparticle drug delivery systems. *J. Pharm. Sci.* 103(1), 29–52 (2014).

54 Via DP, Pons L, Dennison DK, Fanslow AE, Bernini F. Induction of acetyl-LDL receptor activity by phorbol ester in human monocyte cell line THP-1. *J. Lipid Res.* 30(10), 1515–1524 (1989).

55 Arredouani M, Yang Z, Ning Y *et al*. The scavenger receptor MARCO is required for lung defense against pneumococcal pneumonia and inhaled particles. *J. Exp. Med.* 200(2), 267–272 (2004).

56 Tinkle S, Mcneil SE, Mühlebach S *et al*. Nanomedicines: addressing the scientific and regulatory gap. *Ann. N. Y. Acad. Sci.* 1313(1), 35–56 (2014).

57 Farr S, Kellaway I, Parry-Jones D, Sg W. 99m-technetium as a marker of liposomal deposition and clearance in the human lung. *Int. J. Pharm.* 26(3), 303–316 (1985).

58 Gaspar MM, Bakowsky U, Ehrhardt C. Inhaled liposomes – current strategies and future challenges. *J. Biomed. Nanotechnol.* 4, 245–257 (2008).

59 Lehofer B, Bloder F, Jain PP *et al*. Impact of atomization technique on the stability and transport efficiency of nebulized liposomes harboring different surface characteristics. *Eur. J. Pharm. Biopharm.* 88(3), 1076–1085 (2014).

60 Beck-Broichsitter M, Rieger M, Reul R, Gessler T, Seeger W, Schmehl T. Correlation of drug release with pulmonary drug absorption profiles for nebulizable liposomal formulations. *Eur. J. Pharm. Biopharm.* 84(1), 106–114 (2013).

61 Unida S, Ito Y, Onodera R, Tahara K, Takeuchi H. Inhalation properties of water-soluble drug loaded liposomes atomized by nebulizer. *Asian J. Pharm. Sci.* 11, 205–206 (2016).

62 Elhissi AM, Giebultowicz J, Stec AA *et al*. Nebulization of ultradeformable liposomes: the influence of aerosolization mechanism and formulation excipients. *Int. J. Pharm.* 436(1), 519–526 (2012).

63 Murata M, Nakano K, Tahara K, Tozuka Y, Takeuchi H. Pulmonary delivery of elcatonin using surface-modified liposomes to improve systemic absorption: polyvinyl alcohol with a hydrophobic anchor and chitosan oligosaccharide as effective surface modifiers. *Eur. J. Pharm. Biopharm.* 80(2), 340–346 (2012).